BUTTERWORTH HEINEMANN

Polymer Vol. 36 No. 23, pp. 4371–4378, 1995

0032-3861/95/$10.00+0.00

polymer papers

Contact ion pair formation and ether oxygen coordination in the polymer electrolytes $M[N(CF_3SO_2)_2]_2PEO_n$ for M = Mg, Ca, Sr and Ba

Albert Bakker, Shridhar Gejji, Jan Lindgren* and Kersti Hermansson
Institute of Chemistry, Uppsala University, Box 531, S-751 21 Uppsala, Sweden

and Michael M. Probst
Institute of General, Inorganic and Theoretical Chemistry, Innsbruck University, Innrain 52a, A-6020 Innsbruck, Austria
(Received 29 November 1994; revised 23 February 1995)

The polymer electrolytes $M[N(CF_3SO_2)_2]_2PEO_n$ for M = Mg, Ca, Sr and Ba have been investigated using infra-red spectroscopy, differential scanning calorimetry and impedance spectroscopy. The effects of varying concentration ($n = 6$–40) and temperature (25–95°C) on the contact ion pair formation and cation coordination have been studied. Contact ion pairs are only found for the most concentrated samples ($n < 9$). Ion pairs occur with two types of structures: one type is found for samples containing Mg^{2+} and the other for samples with Ca^{2+}, Sr^{2+} and Ba^{2+}. The conductivities of the samples are discussed in terms of radii and coordination numbers of the cations.

(Keywords: polymer electrolytes; contact ion pair formation; cation coordination)

INTRODUCTION

It has been found that poly(ethylene oxide) (PEO) can dissolve a wide variety of ionic salts to form solid polymer electrolytes. These systems show significant ionic conductivity in their amorphous regions, making them potentially important as electrolyte materials in secondary batteries. Most work in the field of polymer electrolytes has dealt with monovalent ions and, in particular, with lithium ions. The use of multivalent cations provides a new possibility to study fundamental properties responsible for ion mobility in polymer electrolytes and might offer new technological applications where lower-cost materials and metals less reactive than lithium are desirable.

The conductivity properties of the polymer electrolyte materials depend directly on the aggregation and mobility of the ions present. Di- and trivalent cations are generally expected to form ion pairs and higher aggregates more readily than monovalent cations, leading to a lower ionic conductivity[1]. Moreover, long-chain polymers like PEO show a tendency to form crystalline phases, where the conductivity is negligible compared to the amorphous parts of the polymer electrolyte. An important concern is therefore to minimize the presence of crystalline phases.

In order to reduce both the ion pairing (i.e. contact ion pairing) and the formation of a crystalline phase, Armand *et al.*[2,3] have produced a series of new anions including bis(trifluoro methane sulfone)imide ('imide'), $[N(CF_3SO_2)_2]^-$. These very flexible anions have a plasticizing effect and reduce the tendency for crystallization, therefore they lower the glass transition of the materials. Moreover, the negative charge is spread out over several atoms and the ion pairing tendency is diminished; in addition, good thermal and chemical stability is obtained.

Details about the molecular-level mechanisms underlying the ionic conductivity are still largely unknown, as are the details about the ion–PEO structures and the ionic aggregates formed. In the present work we have made a systematic study of the $M[N(CF_3SO_2)_2]_2PEO_n$ systems, with M = Mg, Ca, Sr and Ba and $n = 6$–40, using Fourier transform infra-red (*FT*i.r.) spectroscopy, differential scanning calorimetry (d.s.c.) and conductivity measurements.

EXPERIMENTAL

Preparation of the PEO electrolyte films

All studies were carried out with commercial PEO (^{L}PEO, $M_W = 4 \times 10^6$, BDH polyox 301). The imide salts were prepared by dissolving the metal carbonate ($MgCO_3$, Ventron; $CaCO_3$, $SrCO_3$, $BaCO_3$, Merck) in a slight excess of an aqueous solution of $HN(CF_3SO_2)_2$. The $HN(CF_3SO_2)_2$ solution was obtained by passing an

* To whom correspondence should be addressed

aqueous solution of $LiN(CF_3SO_2)_2$ (3M Ltd) through a column containing a cation exchange resin ('Amberlite' IR-120 (Na), BDH). The $M[N(CF_3SO_2)_2]_2$ (with M = Mg, Ca, Sr and Ba) solution was filtered and then precipitated at 100°C. The imide salts were finally dried in vacuum at 140°C for 24 h.

Polymer electrolyte $M[N(CF_3SO_2)_2]_2PEO_n$ films with an ether oxygen/metal ion ratio (n) of 6, 9, 12, 16, 24 and 40 were prepared by the mutual solvent method. The polymer was first dissolved in anhydrous acetonitrile, CH_3CN (Merck, 'for spectroscopy'), the salt dissolved in acetonitrile was then added, and finally, after sufficient mixing, the solutions were cast onto Teflon™ plates for the conductivity measurements, into aluminium pans for the d.s.c. measurements and onto KRS-5 windows for the *FT*i.r. studies. The films were dried under vacuum at 95–100°C for a minimum of 48 h. All preparations and manipulations were carried out under an anhydrous nitrogen atmosphere ($H_2O < 1$ ppm). Once dry and solvent-free, these films were stored at 25°C for at least a week and were not used until any crystallization was complete. From d.s.c. measurements we know that all films were totally amorphous, at least in the composition range $n = 7$–11 (this is in contrast to the corresponding polymer electrolytes with triflates as the anion, i.e. $M(CF_3SO_3)_2PEO_n$, with M = Mg, Ca[4,5], Sr, Ba, which are highly crystalline at room temperature[6]). It was found that no phase changes occurred for a period of more than two months. The films intended for conductivity or d.s.c. measurements were normally 100–200 μm thick. The films to be used in the *FT*i.r. experiments were 10–20 μm thick (determined interferometrically) and their water content was checked from the O–H stretching bands.

D.s.c. measurements

Films of approximately 10 mg were sealed into 40 μl aluminium pans and transferred into a Mettler model DSC20 oven, connected to a Mettler TA4000 controller. During all thermal analyses, a flow of nitrogen was maintained over the perforated pan to keep away atmospheric moisture and remove any decomposition products. The samples were analysed between −150 and 200°C using a heating rate of 10°C min^{-1}.

Conductivity measurements

The conductivities of the polymer electrolytes were determined by a.c. impedance measurements over a frequency range of 2 MHz to 60 Hz with an applied signal of 10 mV by a Solartron 1260 frequency response analyser. Measurements were carried out in the temperature range 25–95°C at approximately 5°C intervals and were controlled by a processor which also operates the frequency analyser and the data acquisition. Stainless steel electrodes were used in a closed cell filled with nitrogen, and thermostated by circulating water through the mounting stage of the cell.

FT*i.r. measurements*

The measurements were recorded on a Digilab-Biorad FTS-45 FT-IR spectrometer covering the range 400–4400 cm^{-1} with a resolution of 1 cm^{-1}. The KRS-5 window was enclosed in a vacuum cell equipped with a heating element. Spectra were recorded between 25 and 95°C.

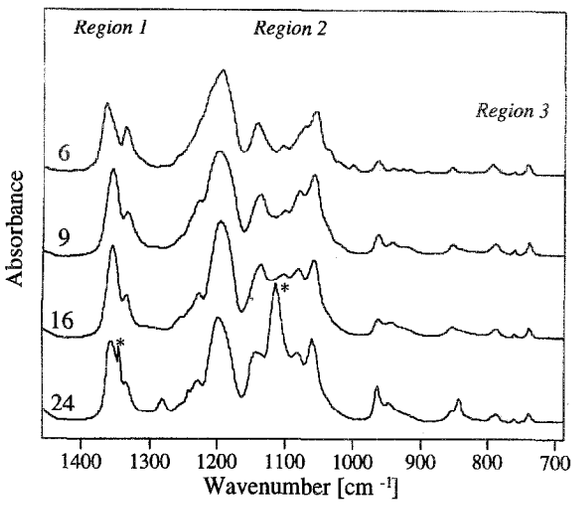

Figure 1 *FT*i.r. absorption spectra of $Mg[N(CF_3SO_2)_2]_2PEO_n$ for $n = 6$, 9, 16 and 24 at 25°C. Dominant crystalline PEO bands are denoted by an asterisk

RESULTS AND DISCUSSION

FT*i.r. spectroscopy*

The *FT*i.r. studies presented here mainly concern the wavenumber region 700–1500 cm^{-1}. *Figure 1* shows overview spectra of $M[N(CF_3SO_2)_2]_2PEO_n$ with M = Mg, and $n = 6$, 9, 16 and 24. The discussion will focus on three sections of these spectra: region 1 at 1333–1355 cm^{-1}, region 2 at 1085–1106 cm^{-1} and region 3 at 710–810 cm^{-1}. Regions 1 and 3 provide information about the coordination of the cation to the imide ion, while region 2 concerns coordination of the cation to the ether oxygens.

For the $Mg[N(CF_3SO_2)_2]_2PEO_{24}$ sample in *Figure 1*, the crystalline PEO phase is observed as a sharp band at 1343 cm^{-1} and a broader one centred at 1116 cm^{-1} (ref. 7). The same bands also appear in the spectra of the electrolytes containing the other cations at the same ether oxygen to cation ratio. No crystalline PEO bands are observed for $n \leqslant 16$. In our d.s.c. measurements (see below) a mixture of crystalline PEO and an amorphous phase was present for $n = 16$ and $n = 24$. The kinetics in the *FT*i.r. films thus appears to be rather slow as compared to the thicker films used for the d.s.c. measurements, leading to supersaturated *FT*i.r. samples. In the case of $Ba[N(CF_3SO_2)_2]_2PEO_6$, a crystalline complex was observed by d.s.c., but no indication of such a complex was seen in the *FT*i.r. spectra.

Ether oxygen coordination. Studies[7] of polycrystalline and amorphous PEO have shown bands at 1148 and 1106 cm^{-1}. The first band (if present) is difficult to distinguish in our spectra, because of the overlap with an imide band. The second band is the C–O–C antisymmetric stretching mode, $\nu(COC)_a$, which shifts to lower wavenumbers when salt is added. This shift indicates a change of the environment of the ether oxygens caused by their coordination to the cations. This phenomenon was discussed in detail in ref. 8, where large shifts were observed for the trivalent rare earth ions. In the present study, the largest shift is observed for M = Mg, with $\nu(COC)_s$ at 1080 cm^{-1}, while in the cases of Ca, Sr and Ba the changes are smaller, with peaks

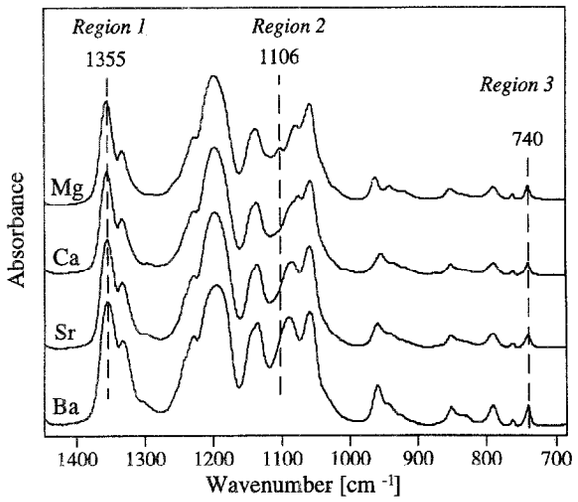

Figure 2 *FT*i.r. absorption spectra of $M[N(CF_3SO_2)_2]_2PEO_9$ for M = Mg, Ca, Sr and Ba, at 25°C

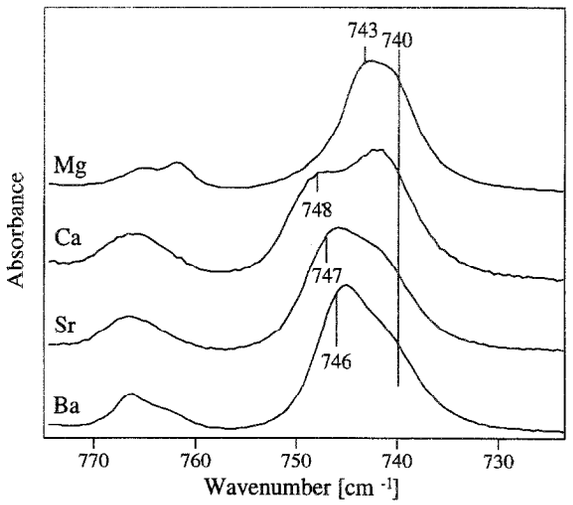

Figure 3 *FT*i.r. absorption spectra of $M[N(CF_3SO_2)_2]_2PEO_6$ for M = Mg, Ca, Sr and Ba, at 25°C. The bands at $\sim 762\,cm^{-1}$ correspond to the C–S stretching mode and the bands at $\sim 740\,cm^{-1}$ to the S–N stretching mode

observed at 1083, 1085 and 1086 cm^{-1}, respectively (see *Figure 2*). The latter is difficult to distinguish from the undisturbed C–O–C vibrational band at 1106 cm^{-1}. A reasonable explanation for the different shifts is that the ether oxygens experience a stronger interaction with a smaller cation, such as Mg^{2+}, leading to a larger shift of the C–O–C vibrational band.

For $n \leqslant 9$, only coordinated PEO is found for M = Ca, Sr and Ba (see *Figure 2*). However, at the salt concentration ($n = 6$), the sample containing Mg^{2+} shows both coordinated and non-coordinated ether oxygens. This indicates that the small Mg^{2+} cation is not able to coordinate all the ether oxygens, despite the fact that there are six ether oxygens available per cation and the usual coordination number for Mg^{2+} is six, as known from numerous diffraction studies done on Mg^{2+} in aqueous solutions and crystalline hydrates. This low number of coordinated ether oxygens can be explained by the formation of ion pairs with the imide ion.

Vibrations of the imide ion. No assignment of the normal vibrations of the imide ion exists in the literature. In our assignments we will therefore use the result of recent *ab initio* molecular orbital calculations made for the free imide ion and for 1 : 1 complexes with the lithium ion[9]. The highest wavenumber band at $\sim 1355\,cm^{-1}$ (in region 1, *Figures 1* and *2*) is an S–O stretching band from the SO_2 groups. In region 3 the molecular orbital calculations predict three bands which are easily recognized in the spectra since rather large gaps occur on both sides of them. The band at $\sim 789\,cm^{-1}$ is a combination of a C–S and an S–N stretching, the one at $\sim 762\,cm^{-1}$ is mainly a combined C–S and C–F stretching, and the band at $\sim 740\,cm^{-1}$ is predominantly an S–N stretching band. Both in the calculations and in the measured spectra, the band at $\sim 740\,cm^{-1}$ was found to be particularly sensitive to ion pair formation. In the next sections we will therefore use the 740 cm^{-1} band as a probe for ion–ion interactions.

Cation effects and ion pairing. *FT*i.r. spectra from Mg^{2+}, Ca^{2+}, Sr^{2+} and Ba^{2+} imides in PEO with concentration $n = 6$ are shown in *Figure 3* for the frequency range of region 3. Since the S–N stretching vibration at $\sim 740\,cm^{-1}$ is non-degenerate, the appearance of distinct components in the experimental profile (*Figure 3*) indicates different environments for the anion. For all the samples with $n > 9$ the band is practically independent of salt concentration or cation type. For the samples with concentrations $n = 6$, bands appear at $\sim 746\,cm^{-1}$ (M = Ba), $\sim 747\,cm^{-1}$ (M = Sr), $\sim 748\,cm^{-1}$ (M = Ca) and at $\sim 743\,cm^{-1}$ (M = Mg). For M = Ba and Sr very small bands are present and for M = Mg and Ca practically no bands are present at these wavenumbers for $n = 9$. The band at $\sim 740\,cm^{-1}$ is attributed to 'free' imide anions. Because the anion is only weakly interacting with the polymer chain in polymer–salt complexes, the observed perturbations of the S–N stretching mode are most likely due to anions paired with cations. For M = Ca, Sr and Ba, the shift of the ion pair component increases for decreasing cation radius. This is expected, since the Coulomb attraction of the cation of smaller size causes a larger perturbation of the anion vibrational mode. However, for M = Mg this shift is relatively small. This indicates a different type of ion–ion coordination for M = Mg as compared to the samples containing the larger cations. The formation of a different type of ion pair for Mg^{2+} is supported by observations done at $\sim 1355\,cm^{-1}$ for $\nu(SO_2)$ vibrations. A band at 1355 cm^{-1} is found for samples with $n \geqslant 9$, independent of cation type (see *Figure 1*). For higher salt concentrations a new component is increasing, downshifted to 1352 cm^{-1} for Ca, to 1350 cm^{-1} for Sr, and to 1347 cm^{-1} for Ba. However, in the case of Mg, an upshift to 1364 cm^{-1} is observed (*Figure 1*), indicating a different type of imide coordination compared to the other cations. In the molecular orbital calculations done on $Li^+N(CF_3SO_2)_2^-$ (ref. 9), different geometries of the cation–anion pairs were in fact found. *Figure 4* shows the optimized geometries of the two most stable structures of the lithium imide pair. In structure A, which is the global minimum, the cation coordinates in a bidentate fashion to oxygen atoms of different SO_2 groups, forming a six-membered ring; in B there is a bidentate coordination to one nitrogen

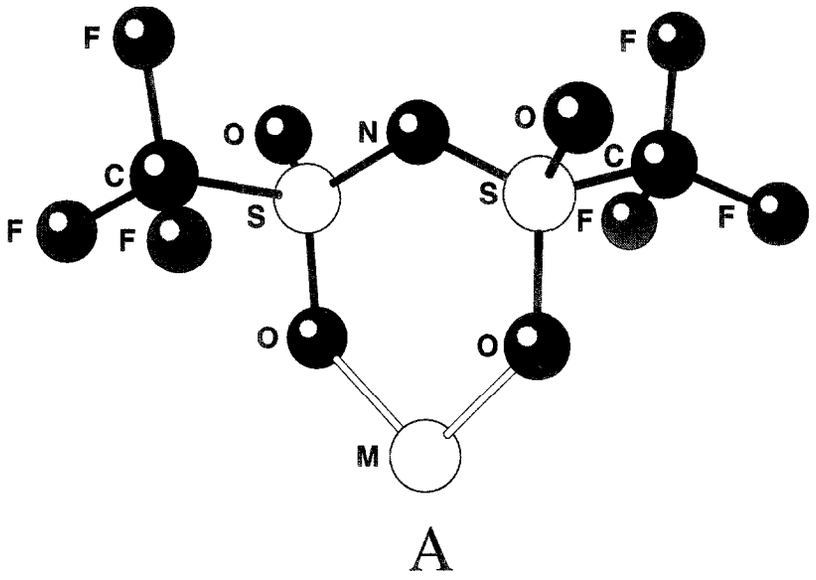

A

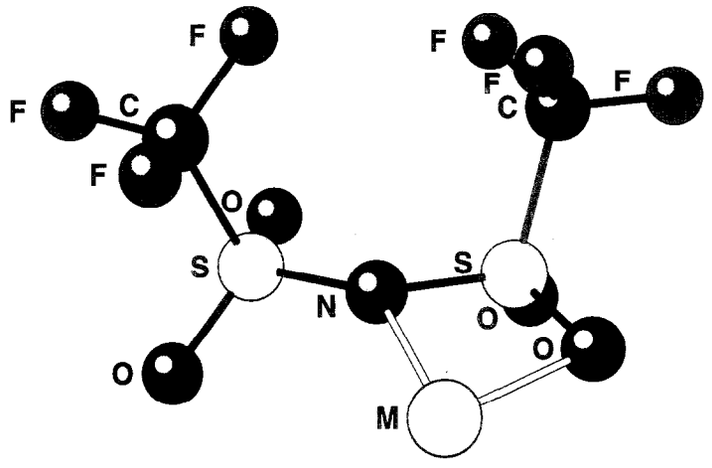

B

Figure 4 Geometry of the metal (M) imide ion pair[8]: (A) coordination of Mg^{2+}; (B) coordination of Ca^{2+}, Sr^{2+} or Ba^{2+}

and one oxygen atom. Normal coordinate analyses done for both structures show that there is a frequency upshift for the S–N stretching band which is considerably larger for structure B than for A. We conclude that contact ion pairs between imide and Mg^{2+} have a structure of type A and pairs involving Ca^{2+}, Sr^{2+} and Ba^{2+} have a structure of type B.

A detailed study of the relative amount and cation dependence of the ion pair formation was performed by means of bandshape analyses of the S–N stretching region for $M[N(CF_3SO_2)_2]_2PEO_n$ for all four cations and with $6 \leqslant n \leqslant 9$. The bandshape analyses were performed assuming Lorentzian functions. Because of the (small) overlap of the C–S with the S–N stretching bands it was necessary to include in the fit the contours of the higher wavenumber C–S bands. These bands were fitted using Gaussian shapes and were included mainly to eliminate any bias on the fitted parameters of the S–N bands. Results from the band fits are displayed in *Figures 5* and *6*; the concentration dependence of the spectra is exemplified by $Ca[N(CF_3SO_2)_2]_2PEO_n$ ($n = 6, 7, 9, 16$) in *Figure 5* and the ion-type dependence by the $M[N(CF_3SO_2)_2]_2PEO_6$ (M = Mg, Ca, Sr, Ba) spectra in *Figure 6*. The mode at $740\,cm^{-1}$, present in all spectra, was above assigned to 'free' imide ions, and is indeed independent of cation type and concentration, as expected for the vibration of a 'free' anion. The higher frequency Lorentzian band, assigned above to ion pairs, is frequency-independent with respect to salt concentration, but varies in height, as seen in *Figure 5*. The amount of ion pairs decreases rapidly as n increases from 6 to 9, where virtually all the cations are solvated by the PEO oxygens. This is observed for all the cation types. The increase in number of ion pairs for the larger cations among Ca^{2+}, Sr^{2+} and Ba^{2+} (*Figure 6*) is probably caused by the decrease of the stability between the polar

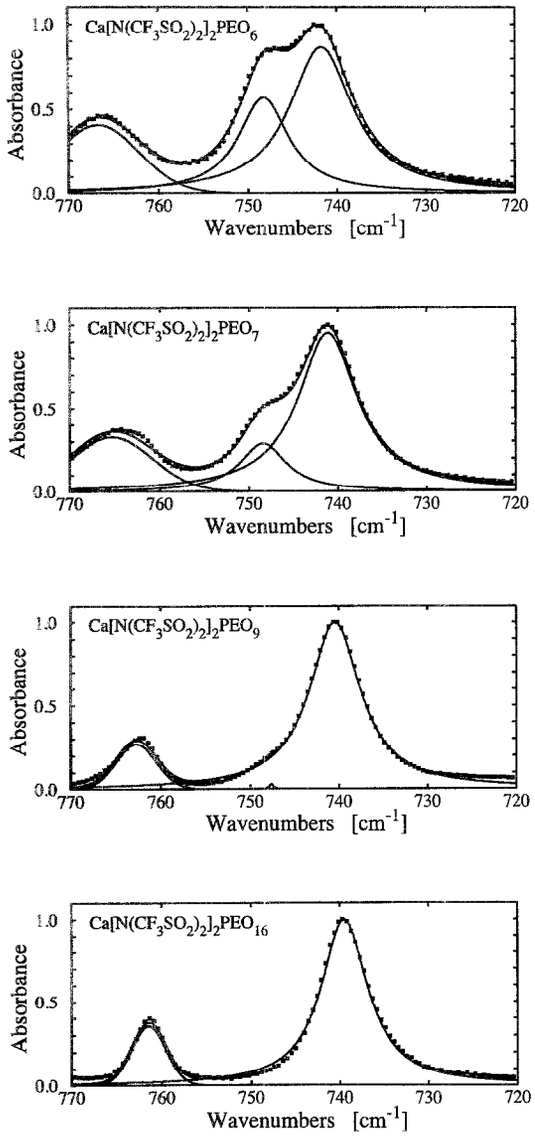

Figure 5 The S–N stretching mode at $\sim 740\,cm^{-1}$ (uncoordinated imide) and at $\sim 748\,cm^{-1}$ (coordinated imide) of $Ca[N(CF_3SO_2)_2]_2PEO_n$ for $n = 6$, 7, 9 and 16 at 25°C. For these bands the solid lines correspond to the components of the Lorentzian envelope fitted to the spectrum (dots). The components are attributed to 'free' imide ions and ion pairs. The C–S stretching bands at $\sim 765\,cm^{-1}$ are fitted to Gaussian bandshapes

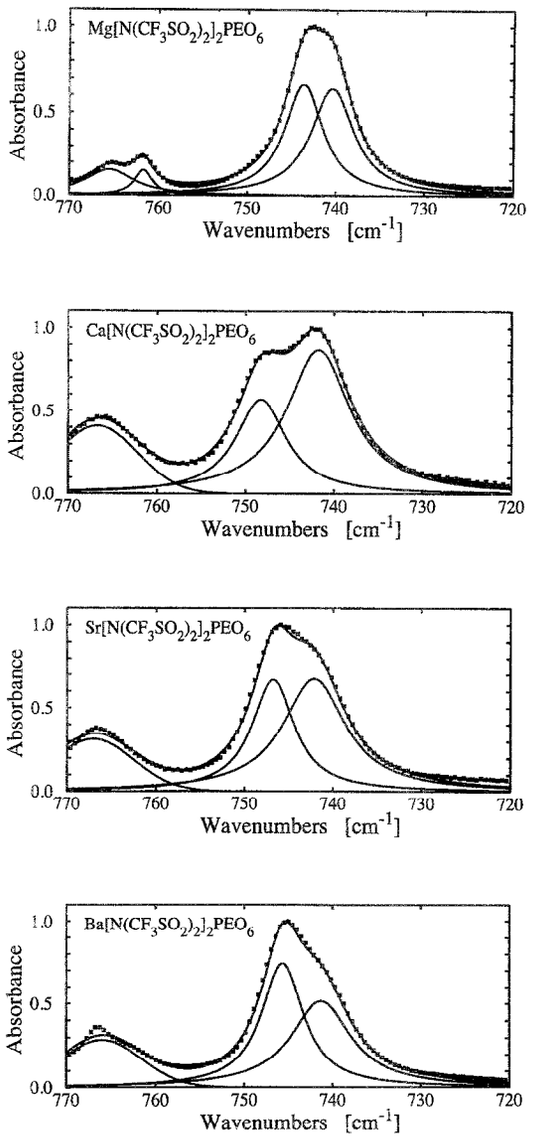

Figure 6 The S–N stretching mode at $\sim 740\,cm^{-1}$ (uncoordinated imide) and at $\sim 748\,cm^{-1}$ (coordinated imide) of $M[N(CF_3SO_2)_2]_2PEO_6$ for M = Mg, Ca, Sr and Ba, at 25°C. The bands are fitted in the same way as those in *Figure 5*

groups in the polymer and the cation, predicted from the hard–soft acid–base principle[10]. The competition between ether oxygen–cation and the anion–cation interactions then favours the formation of ion pairs. The diverging behaviour for Mg^{2+} is probably due to the different ion–ion pair structure.

Temperature effects. It has been stated in the literature that ion pair and cluster formation increases on increasing the temperature[11,12]. This effect is not observed for our samples. Both the S–N stretching and the SO_2 vibrations change very little between 25 and 90°C. A noticeable change was observed for the S–N stretching band for 'free' imide ions. A broadening of the band and a decrease of the peak frequency were observed for increasing temperature and can be related to a decreased conformational order and an increase in the flexibility of the imide ion.

Conductivity measurements

The conductivity data can be modelled with the Vogel–Tammann–Fulcher (VTF) equation[13–15]:

$$\sigma = AT^{-1/2}\exp[-B/(T - T_0)] \qquad (1)$$

where A, B and T_0 are constants. The least-squares fitted values of the three parameters are given in *Table 1* for $n = 9$, 12 and 16. The constant B increases slightly as n increases. Moreover, for the larger cations, B is somewhat larger than for Mg^{2+}. The parameter T_0 is found to be ~ 45°C below the glass transition temperature (T_g), as determined by d.s.c. (see below). This result is not unexpected since $T_g - T_0$ is typically of the order of 45–50°C for polymer electrolyte systems[16,17].

Comparison with samples containing a crystalline complex or crystalline PEO is less significant because ion conduction takes place through the amorphous regions, where the salt concentration is different from the nominal value. To discuss the conductivity results at any defined concentration or ion type it is therefore

Table 1 Parameters describing fits to the equation $\sigma = AT^{-1/2}\exp[-B/(T-T_0)]$ for conductivity data for the $M[N(CF_3SO_2)_2]_2PEO_n$ complex salts with M = Mg, Ca, Sr and Ba and $n = 9$, 12 and 16

Electrolyte M	n	$^{10}\log A$	B (K)	T_0 (K)
Mg	9	1.15	1286	217
	12	0.93	1226	197
	16	2.99	2212	160
Ca	9	1.15	1238	224
	12	1.05	1069	222
	16	2.80	2272	155
Sr	9	1.11	1419	216
	12	3.01	2512	161
	16	2.68	2296	152
Ba	9	2.08	1731	218
	12	1.85	1539	213
	16	2.86	2356	156

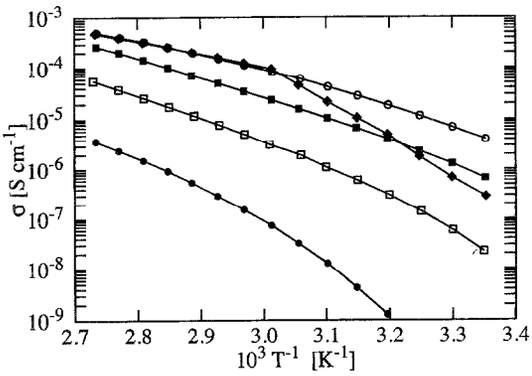

Figure 7 Logarithm of the total conductivity of $Sr[N(CF_3SO_2)_2]_2PEO_n$ samples for $n = 6$ (●), 9 (□), 12 (■), 16 (○) and 24 (◆)

necessary to compare only amorphous samples or conductivity data from above the melting temperature of PEO. In *Figure 7* the conductivities for the $Sr[N(CF_3SO_2)_2]_2PEO_n$ samples with compositions $n = 6$–24 are plotted as $\ln\sigma$ vs. $10^3/T$. Within this composition range, the conductivity increases on decreasing salt concentration. The behaviour of the other samples is analogous to that of M = Sr. The vibrational analyses above showed that no ion pairs or higher aggregates are left for compositions $n > 9$. This means that we can concentrate on other factors in order to understand and explain the observed conductivities. Segmental motion has been suggested for a long time as a component of the conduction mechanism in polymer electrolyte systems[18]. It has been shown recently that the correlation time of the segmental motion in PEO is greatly reduced on dissolving a salt in the polymer[19–21]. This was explained by the formation of cation–ether oxygen bonds to ether oxygens either within the same chain or via crosslinks to other chains.

Recently[22–24], the conductivities and glass transition temperatures of alkali metal imides dissolved in PEO(4000) have been investigated. A weak dependence on cation size was found and was discussed in terms of cation–ether binding energy and cation coordination number. The influence of cation type on conductivity in the present case has been studied for $n = 6$–40 and the

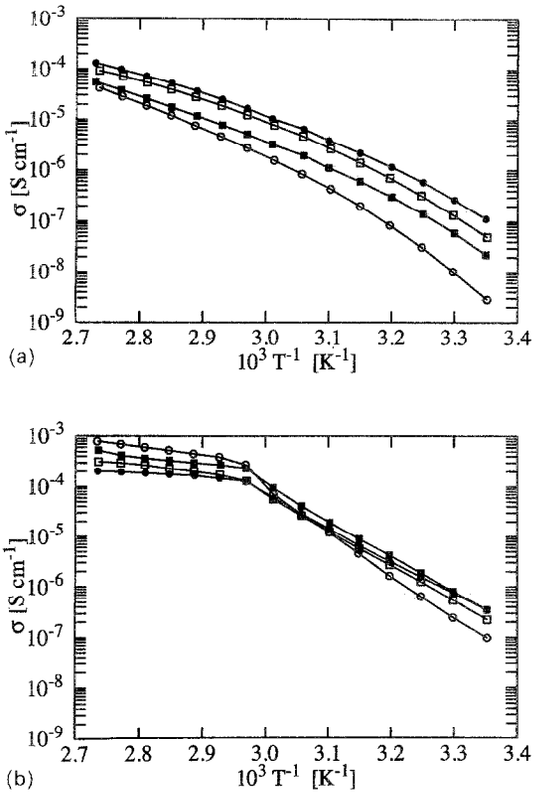

Figure 8 Logarithm of the total conductivity of $M[N(CF_3SO_2)_2]_2PEO_n$ for M = Mg (●), Ca (□), Sr (■) and Ba (○) and $n = 9$ (a) and 40 (b)

results are illustrated in *Figure 8* for samples of composition $n = 9$ (a) and 40 (b) for M = Mg, Ca, Sr and Ba. For $n = 9$ the highest conductivities are obtained for samples containing cations with the smallest radii throughout the temperature range measured. The same effect is observed for samples with compositions $n = 9$–12 but the difference gradually diminishes for the more dilute samples. For $n = 24$ and 40, a reversal of the order has been obtained and the conductivities are systematically larger for the larger cations, as seen for the amorphous cases, namely for temperatures above the melting point of PEO (*Figure 8b*). The variations in the conductivity can be explained by identifying two main factors which control the ionic mobility. Firstly, cations with smaller radii exhibit stronger interaction with the ether oxygens of the polymer backbone, resulting in more inert bonds which decrease the mobility of the cations and the conductivity. Secondly, smaller cations are expected to coordinate fewer of the ether oxygens and therefore more ether oxygens will be left uncoordinated at a given composition. This is expected to result in faster average segmental motions for the smaller cations. These two factors influence the conductivity in different directions and the second factor, the difference in the number of ether oxygens coordinated by the cations, can be expected to dominate at high salt concentrations. The first factor, the difference in bond lability, can be expected to increase in importance at lower salt concentrations.

The samples with $n = 6$ are amorphous for M = Mg, Ca and Sr. The conductivity of the sample with M = Mg is exceptionally low compared to samples with M = Ca or Sr.

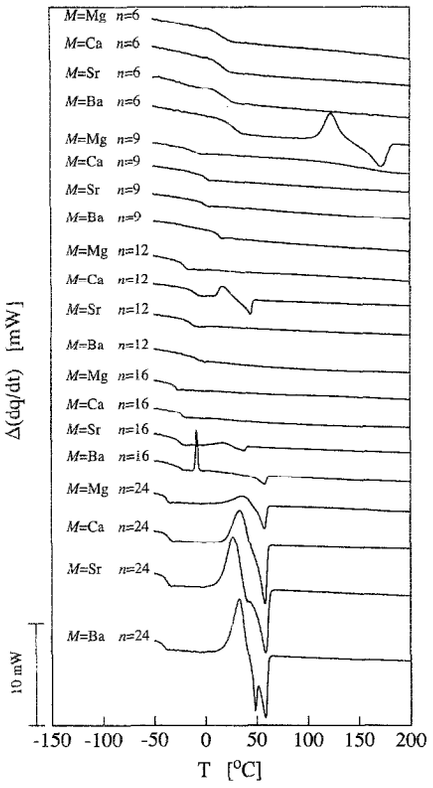

Figure 9 D.s.c. traces of $M[N(CF_3SO_2)_2]_2PEO_n$ samples during the second heating cycle

Comparison with d.s.c. measurements

D.s.c. thermograms for $M[N(CF_3O_2)_2]_2PEO_n$ with M = Mg, Ca, Sr and Ba and $n = 6$, 9, 12, 16 and 24 are shown in *Figure 9* during the second heating cycle. The exothermal peaks indicate non-equilibrium conditions in some of the samples at low temperatures, and do not appear during the first heating cycle. Investigation of the d.s.c. traces shows that the samples are highly amorphous within a broad range of compositions, as they exhibit only a glass transition. For lower salt concentrations ($n = 24$), crystallization of the pure polymer host occurs. As observed in the figure, the glass transition temperature (taken at the mid-point of the inflection) is dependent on the salt concentration, a common phenomenon in polymer electrolytes. For the samples with $n = 9$–16, T_g is lowest for those containing Mg^{2+}. For $n = 9$, a variation of T_g from −12.8°C for Mg^{2+} to +7.6°C for Ba^{2+} is obtained, as shown in *Figure 10*. The reason for the lower T_g for Mg^{2+} is probably that a lower ether oxygen coordination number leads to a larger chain motion, as discussed above. For $n = 6$, an increase in the width of the glass transition temperature is observed and is attributed to a more disordered structure of the polymer chains[25].

CONCLUSIONS

It has been demonstrated that quantitative determinations of the cation–anion interactions can be obtained from *FT* i.r. data. Ion pairs appear to play a minor role in the polymer electrolytes based on PEO and the divalent imide salts considered in this study. Ion pairs appear only for electrolytes with compositions $n < 9$. This is in fact the expected behaviour, as mentioned in the Introduction. Two types of ion pair complexes are found in the highly concentrated systems: the cation forms bidentate structures either with oxygen atoms of both SO_2 groups of the imide ion (for M = Mg) or with the N and O atoms (for M = Ca, Sr and Ba).

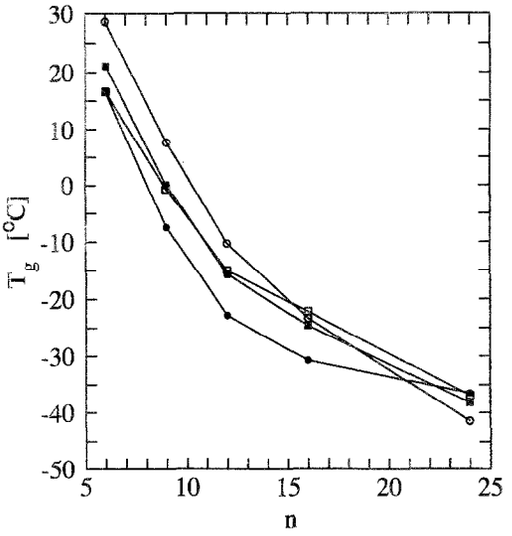

Figure 10 Glass transition temperature (T_g) for samples $M[N(CF_3SO_2)_2]_2PEO_n$ for M = Mg (●), Ca (□), Sr (■) and Ba (○) and $n = 6$, 9, 12, 16 and 24

We find, through examination of samples with compositions $n = 9$–40, that the difference between the conductivities of electrolytes of the same composition is controlled either by the coordination number of the cation ($n \approx 9$–12) or the lability of the cation–polymer bond ($n > 16$). The difference in coordination number also explains why the samples containing Mg^{2+} have the lowest glass transition temperature for $n = 9$–12.

ACKNOWLEDGEMENT

This work was supported by the Swedish Natural Science Research Council, the Swedish Research Council for Engineering Sciences and a SCIENCE grant from the EEC (grant number ERBSC1*CT000567-(SC1000567)). We would also like to thank Dr J. Prud'homme for providing a preprint of work submitted for publication and Dr Jörgen Tegenfeldt for fruitful discussions.

REFERENCES

1 Farrington, G. C. and Linford, R. G. 'Polymer Electrolyte Reviews—2' (Eds J. R. MacCallum and C. A. Vincent), Elsevier Applied Science, London, 1989, pp. 255–283
2 Armand, M., Gorecki, W. and Andréani, R. 'Second International Symp. on Polymer Electrolytes' (Ed. B. Scrosati), Elsevier Applied Science, London, 1990, p. 91
3 Armand, M., Gaulthier, M. and Muller, D. US Patent 5,021,308, 1991
4 Mehta, M. A. PhD Dissertation, University of St. Andrews, 1992
5 Bruce, P. G. and Vincent, C. A. *J. Chem. Soc. Faraday Trans.* 1993, **89**, 3187
6 Bakker, A., Lindgren, J. and Hermansson, K. *Polymer* (in press)
7 Wendsjö, Å., Lindgren, J. and Paluszkiewicz, C. *Electrochim. Acta* 1992, **37**, 1689
8 Bernson, A. and Lindgren, J. *Solid State Ionics* 1993, **60**, 31

9 Gejji, S. P., Lindgren, J., Tegenfeldt, J. and Hermansson, K. (in press)
10 Pearson, R. G. *J. Am. Chem. Soc.* 1963, **85,** 3533
11 Torell, L. M. and Schantz, S. 'Polymer Electrolyte Reviews—2' (Eds J. R. MacCallum and C. A. Vincent), Elsevier Applied Science, London, 1989, p. 1.
12 Wendsjö, Å., Lindgren, J. and Thomas, J. O. *Solid State Ionics* 1992, **53–56,** 1077
13 Vogel, H. *Phys. Z.* 1921, **22,** 645
14 Tammann, G. and Hesse, W. Z. *Anorg. Allg. Chem.* 1926, **156,** 245
15 Fulcher, G. S. *J. Am. Ceram. Soc.* 1925, **8,** 339
16 Angell, C. A. *Solid State Ionics* 1983, **9–10,** 3
17 Greenbaum, S. G., Pak, Y. S., Wintersgill, M. C., Fontanella, J. J., Schultz, J. W. and Andeen, C. G. *J. Electrochem. Soc.* 1988, **135,** 235
18 Ratner, M. 'Polymer Electrolyte Reviews—1' (Eds J. R. MacCallum and C. A. Vincent), Elsevier Applied Science, London, 1989, p. 173
19 Berthier, C., Gorecki, W., Minier, M., Armand, M. B., Chabagno, J. M. and Rigaud, P. *Solid State Ionics* 1983, **11,** 91
20 Johansson, A., Wendsjö, Å. and Tegenfeldt, J. *Electrochim. Acta* 1992, **37,** 1487
21 Johansson, A. and Tegenfeldt, J. *Macromolecules* 1992, **25,** 4712
22 Besner, S. and Prud'homme, J. *Macromolecules* 1989, **22,** 3029
23 Besner, S., Vallée, A., Bouchard, G. and Prud'homme, J. *Macromolecules* 1992, **25,** 6480
24 Perrier, M., Besner, S., Paquette, C., Vallée, A. and Prud'homme, J. *Electrochim. Acta* (submitted)
25 Bershtein, V. A. and Egorov, V. M. 'Differential Scanning Calorimetry of Polymers', Ellis Horwood, Chichester, 1994